

# Combination of pembrolizumab and <sup>125</sup>I attenuates the aggressiveness of non-small cell lung cancer

SHUO WANG, JUN ZHANG, FAN-JIE MENG, YI-JIE YAN, BIN WANG and ZHI-YU GUAN

Department of Thoracic Surgery, The Second Hospital of Tianjin Medical University, Tianjin 300211, P.R. China

Received May 9, 2019; Accepted November 14, 2019

DOI: 10.3892/ol.2020.11508

**Abstract.** Non-small cell lung cancer (NSCLC) is the leading cause of cancer-associated mortality. Therapies targeting programmed cell death 1 ligand 1 (PD1L1) have promising effects on NSCLC. However, resistance to targeted therapy has become the main problem and the underlying molecular mechanism remains unclear. In the present study, the expression of PD1L1 in NSCLC was determined and the association with clinicopathological characteristics was analyzed. A combination therapy was also constructed, including pembrolizumab (Pem) and iodine-125 (<sup>125</sup>I), which represented an efficient strategy for the treatment of NSCLC. The expression of PD1L1 was upregulated in NSCLC tissues and positively correlated with the Ki-67 index, pathological subtypes and risk stages. A higher level of PD1L1 expression was associated with poorer survival in patients with NSCLC, which could be used as a prognostic indicator. When NSCLC cells were cultured in the presence of Pem and <sup>125</sup>I seeds, the combination treatment significantly abrogated the tumor proliferation and aggressiveness through the inhibition of matrix metalloproteinase-2 and -9 secretion. Flow cytometry analysis revealed pembrolizumab combined with <sup>125</sup>I contributed to a higher rate of apoptosis and cell cycle arrest, indicating that the combination treatment improved the resistance to immunotherapy. Furthermore, the associated molecular mechanism was the dysregulation of ADAM metalloproteinase domain 17. The findings from the present study revealed that PD1L1 could be used as a predictive biomarker, and the application of combination treatment of pembrolizumab and <sup>125</sup>I showed promising effects on NSCLC.

## Introduction

Lung cancer accounts for ~1.8 million patients and led to 1.6 million deaths globally by 2015 (1,2), which is the most common cause of cancer-related death in males and the second most common cause in females (3). A majority of patients are diagnosed at ~70 years old. Overall, only 17.4% of patients with lung cancer in the USA survive >5 years following the initial diagnosis (4), while the outcomes, on average, are worse in the developing world ~10.6% (5). Lung cancers are classified based on histology (6), which is important to determine both management and prognostic prediction. The three main subtypes of non-small cell lung cancer (NSCLC) include adenocarcinoma, squamous-cell carcinoma and large-cell carcinoma (7). In spite of the significant advance in diagnostic and therapeutic strategies, the resistance to existing therapies still remains a huge challenge.

A recent clinical trial has reported that anti-programmed cell death protein-1 (PD-1) and programmed cell death 1 ligand 1 (PD1L1) antibodies have produced a clinical response and survival improvement in advanced NSCLC (8). Furthermore, two reagents, pembrolizumab (Pem) and nivolumab, have been approved by the USA Food and Drug Administration (FDA) for the treatment of advanced NSCLC (9,10). Although targeting PD1L1/PD-1 has displayed promising effects on NSCLC, the two reagents offer little improved outcomes due to the resistance to immunotherapy drugs among more than one-third of patients with a high level of PD1L1 expression (8,11). This phenomenon has become the bottleneck in clinical practice. Thus, the exploration of underlying mechanism of resistance will maximize the application of immunotherapy in NSCLC and in addition, facilitate bedside-to-bench studies in other types of cancer immunotherapy, such as breast and prostate cancers. Comprehensive treatment plays a critical role in NSCLC, including chemotherapy, immunotherapy and radiation. Nevertheless, it is difficult to deliver a sufficient radiation dose to tumors using external beam radiotherapy alone because of the obstruction of surrounding tissues (12). Radioactive seed implantation has been reported to be successfully applied for treating inoperable solitary lung cancers, while avoiding excessive radiative exposure to surrounding normal tissues (13), such as iodine-125 (<sup>125</sup>I) seed implantation. However, there still remains illusive whether <sup>125</sup>I radiation can improve the resistance of NSCLC to immunotherapy. Therefore, the current study aimed to explore an approach to

*Correspondence to:* Professor Zhi-Yu Guan, Department of Thoracic Surgery, The Second Hospital of Tianjin Medical University, 23 Pingjiang Road, Tianjin 300211, P.R. China  
E-mail: guanzy69@163.com

*Abbreviations:* PD1L1, programmed cell death 1 ligand 1; ADAM17, ADAM metalloproteinase domain 17; RT-qPCR, reverse transcriptase-quantitative polymerase chain reaction; PI, propidium iodide; MMP, matrix metalloproteinase; FCM, flow cytometry

*Key words:* non-small cell lung cancer, programmed cell death 1 ligand 1, iodine-125, targeted therapy

improve the resistance to immune checkpoint therapy. To the best of our knowledge, it is the first study to detect the effects of combination therapy with PD1L1 inhibitor and  $^{125}\text{I}$  on NSCLC with the goal of improving the resistance to immunotherapy.

## Materials and methods

**Patients and samples.** NSCLC-associated specimens were obtained from 92 patients with NSCLC (50 men; 42 women; mean age 41.2 years, age range 28-76 years) undergoing surgery at the Department of Thoracic Surgery in The Second Hospital of Tianjin Medical University between October 2014 and June 2018. Two experienced pathologists at the Department of Pathology in The Second Hospital of Tianjin Medical University confirmed the diagnosis independently (14). The stained methods have been provided in IHC sections. None of patients had received chemotherapy and radiotherapy before the operation. The patient information, including the general characteristics, diagnosis, treatment strategy and the survival time, were obtained from the medical records or outpatient follow-up records of the patients every 3 months. All of the operative tissues [normal lung (distance to tumor tissues, 2 cm) and tumor tissues] were harvested during resection. Subsequently the samples were immediately frozen with liquid nitrogen and stored until further use. The aforementioned procedures were approved by the Research Ethics Committee of Tianjin Medical University. All patients provided written informed consent in accordance with the Declaration of Helsinki.

**Cell lines.** The human H460, H1299 and A549 NSCLC cell lines, and the PC6 SCLC cell line, were purchased from the Institute of Basic Medical Sciences Peking Union Medical College. The PC6 cells were used as a control. The 4 tumor cell lines were authenticated using cellular morphology and cultured in DMEM (Thermo Fisher Scientific, Inc.) supplemented with 10% FBS (Thermo Fisher Scientific, Inc.) and penicillin/streptomycin (1%) at 37°C in a humidified incubator with 5%  $\text{CO}_2$ . H460 and A549 cell lines in the following experiments were divided into four groups: i) Pem combined with  $^{125}\text{I}$  (Pem +  $^{125}\text{I}$ , 10  $\mu\text{g}/\mu\text{l}$ ); ii) Pem 10  $\mu\text{g}/\mu\text{l}$ ; iii)  $^{125}\text{I}$ , 10  $\mu\text{g}/\mu\text{l}$ ; and iv) DMSO, 10  $\mu\text{g}/\mu\text{l}$ .

**Main reagents.** Pem (5 ml; 20 mg; molecular weight 534.6) was purchased commercially from Merck KGaA.  $^{125}\text{I}$  radioactive seeds with 22.4-29.6 MBq/particle were purchased from Shanghai GMS Pharmaceutical Co. Ltd. Both reagents were stored at -20°C and a small amount (10  $\mu\text{g}/\mu\text{l}$ ) was used for subsequent experiments.

**Immunohistochemical (IHC) staining.** IHC staining procedures were performed according to the manufacturer's instructions. Tissues were dehydrated by using ethanol gradient (70, 80 and 95%; 5 min each), followed by incubation with 100% ethanol three times for 5 min. The paraffin-embedded block was sliced into 5-8  $\mu\text{m}$  thick sections using a microtome and washed in a 40°C water bath containing distilled water for 15 min. Section were fixed in 4% PFA (Image-iT™ Fixation/Permeabilization Kit; Invitrogen; Thermo Fisher Scientific, Inc.) at 4°C overnight. The sections were heated

at 75°C for 30 min and 5% normal FBS (Thermo Fisher Scientific, Inc.) to reduce unspecific background staining. Briefly, to investigate the expression of PD1L1 in lung cancer tissue and investigate the association with tumor proliferation, the prepared sections were stained with anti-PD1L1 antibody (cat. no. CST51296; 1:100; Cell Signaling Technology, Inc.) and anti-Ki-67 antibody (cat. no. AB15580; 1:100; Abcam) at 4°C overnight. The validity of these antibodies has been confirmed by previous studies (15,16). Subsequently, the samples were washed with PBS and incubated with the goat to rabbit secondary antibodies (Thermo Fisher Scientific, Inc.; cat. no. A11034; 1:500) for 1 h at room temperature. The ratio of PD1L1-positive cells and Ki-67-positive cells was calculated by counting the average number of stained cells in 500 nuclei in four random light high-power fields (magnification 400X (17). The average IHC score of PD1L1 in all samples was 6. Histopathological diagnoses were confirmed by two pathologists at The Second Hospital of Tianjin Medical University based on the WHO classification of thorax tumors.

**MTT assay.** To determine cell proliferation, MTT assays were strictly performed according to our previous work (18). The H460 cells (1,000 cells/well) were seeded into 96-well plates for 24 h (37°C, 5%  $\text{CO}_2$ ) and subsequently treated with different compounds (10  $\mu\text{g}/\mu\text{l}$ ) based on the aforementioned groups for an additional 24 h. Cell viability was assessed using the MTT assay. Briefly, 0.5 mg MTT reagent was added to each well for 4 h of incubation before the end of Pem or  $^{125}\text{I}$  treatment. After removing the supernatant, 100  $\mu\text{l}$  DMSO was added to each well and incubated for 10 min. The purple mixture in each well was then measured at 490 nm using the Polarstar Optima microplate reader from BMG Labtech GmbH. The inhibition rate was analyzed using the following formula: [(Control D490-Experimental D490)/Control D490] x100%.

**Flow cytometry (FCM) analysis.** FCM analysis was performed according to the manufacture's instructions. Briefly, tumor cells were diluted to  $1 \times 10^5/\text{ml}$  and treated with the aforementioned reagents, in the four treatment groups for 24 h. The cells were dissociated in 1X binding buffer and subsequently stained with Annexin V-FITC (Biolegend, Inc.) and propidium iodide (PI) in the dark for 20 min at room temperature and analyzed using FCM (Becton, Dickinson and Company) cell sorting. The apoptosis rate was calculated as the percentage of the Annexin V-FITC<sup>+</sup>/PI<sup>+</sup> cells from the total cells. Additionally, the dissociated cells were incubated in 95% cold alcohol overnight at 4°C and then stained with PI (50  $\mu\text{g}/\text{ml}$ ) supplemented with Triton X-100 in the dark for 30 min at 4°C. In total,  $1 \times 10^4$  cells were used as the gate region and analyzed using FCM cell sorting to examine the cell cycle. The dead cells were calculated as the proportion of PI<sup>+</sup> cells. The data is presented as the mean  $\pm$  standard deviation from three independent experiments.

**ELISA.** ELISA was performed using the matrix metalloproteinase (MMP)2 and MMP9 ELISA kits (Boster Biology Technology, cat. nos. EK1488 and EK1107) according to the manufacturer's instructions. Briefly, 100  $\mu\text{l}$  supernatant from H460 and A549HE cells cultured with the aforementioned reagents for 8 h was added into duplicate wells and incubated

at 37°C for 90 min. After washing three times, 100  $\mu$ l indicating antibodies from the ELISA kits were added and incubated at 37°C for 60 min. After the color reaction step with 3,3',5,5'-tetramethylbenzidine substrate for 15 min at 37°C, absorbency was detected at 450 nm using a microplate reader (SpectraMax; Molecular Devices, LLC). The data is presented as the mean  $\pm$  standard deviation from three independent experiments.

**Cell lysis.** Cells from all 4 cell lines were lysed with ice-cold buffer (50 mM Tris, Cl pH 6.8, 15 mM NaCl, 5 mM EDTA, 0.5% NP-40 and 1 mM PMSF) supplemented with 0.1% Triton X-100 and 20 mM Tris-HCl (pH 7.4), and protease-inhibitor cocktail. The protein concentration was determined with Coomassie Brilliant Blue (Thermo Fisher Scientific, Inc.; cat. no. 23200) using a microplate spectrophotometer (Infinite M200 PRO; Tecan Group, Ltd.).

**Western blot analysis.** The total protein (50  $\mu$ g) was separated with 10% SDS-PAGE gel and the protein was transferred on to PVDF membranes. The membranes were subsequently incubated against the Bax (cat. no. AB182733; Abcam) and Bcl-2 (cat. no. AB32124; Abcam) antibodies overnight at 4°C. Subsequently, the membranes were probed with secondary antibodies (cat. no. GL1538; GuideChem; 1:500) for 1 h at room temperature.  $\beta$ -actin was utilized as the loading control. The primary antibodies were diluted to 1:500 and the  $\beta$ -actin antibody was diluted to 1:3,000. The immunoblotting results were visualized using TMB (cat. no. PR1210; Beijing Solarbio Science & Technology Co., Ltd.).

**RNA extraction and reverse transcription-quantitative PCR (RT-qPCR).** RNA was isolated from tumor tissues and cells from all 4 cell lines following the treatment of the aforementioned reagents using TRIzol<sup>®</sup> (Invitrogen; Thermo Fisher Scientific, Inc.), according to the manufacturer's protocol. cDNA was synthesized using iScript reverse transcription system (Invitrogen; Thermo Fisher Scientific, Inc.) and 2  $\mu$ g RNA. Real-time RT-PCR conditions were 95.0°C for 5 min, 35 cycles of 95.0°C for 30 sec and 60.0°C for 30 sec. The mRNA expression levels of PDIL1, p21, p27 and ADAM metalloproteinase domain 17 (ADAM17) were determined using the iQ SYBR Green Supermix kit (Bio-Rad Laboratories, Inc.) and the Bio-Rad iQ5 Multicolor Real-Time PCR detection system and normalized with GAPDH mRNA. The following conditions were used for the qPCR: Initial denaturation at 95.0°C for 5 min, then 35 cycles of 95.0°C for 30 sec and 60.0°C for 30 sec. The  $2^{-\Delta\Delta C_t}$  method (19) was performed to calculate the fold change and all the experiments were conducted three times. The sequences used for the primers are provided in Table SI.

**Statistical analysis.** Student's t-test and  $\chi^2$  test were used to determine the statistical difference between the reagent treatment group and the control group. Data were presented as the means  $\pm$  standard deviation. Data were analyzed by Student's t-test and Mann-Whitney test using SPSS v19.0 (IBM Corp.) and GraphPad Prism v7.0 (GraphPad Software, Inc.). An unpaired t-test was used for comparison between two groups, and comparison of mean values between multiple

groups was evaluated by one-way ANOVA followed by Student-Newman-Keuls post hoc test. The functional experiments were performed at least three times. The correlation between PDIL1 expression and Ki-67 labeling was determined using Pearson's correlation. The clinical risk factors were analyzed using logistic regression. Survival analysis was performed using Kaplan-Meier curves. The Mantel-Cox log-rank test was used to assess the significant differences between survival curves.  $P < 0.05$  was considered to indicate a statistically significant difference.

## Results

*PDIL1 expression is positively correlated with proliferation of NSCLC.* A total of 92 NSCLC cases were included in the present study: 71 (77.17%) were squamous cell carcinoma, 16 (17.39%) were adenocarcinoma and 5 (5.43%) were large cell carcinoma (Table I). The expression of PDIL1 was examined using IHC. PDIL1 was expressed in human NSCLC samples and was located on the surface of tumor cells (Fig. 1A). As presented in Table I, the IHC score of PDIL1 was  $< 6$  in 33 (35.87%) cases and  $> 6$  in 59 (64.13%) samples. The Ki-67 index of the 92 NSCLC cases was determined and the samples were subsequently divided into three groups depending on the percentage of cells stained positive. Ki-67 labeling was identified as low percentage ( $< 10.0\%$ ) in 28 (30.43%) cases, moderate percentage (10.0-20.0%) in 34 (36.96%) cases and high percentage ( $> 20.0\%$ ) in 30 (32.61%) cases. Most of the cases had moderate percentage expression. Similarly, most of the patients (49; 53.26%) were at the second risk stage (Table I). Additionally, the association of PDIL1 expression with Ki-67 index was evaluated by Pearson's correlation, which revealed positive correlation (Fig. 1A). These data suggests that PDIL1 expression was associated with proliferation of NSCLC.

*PDIL1 is a prognostic indicator for patients with NSCLC.* In the present study, the median follow-up time was 35.8 months (range 3.0-59.0 months). Among them, 39 (42.39%) patients were alive and 53 (57.61%) patients died as a result of NSCLC during the follow-up periods. In addition, among the patients (dead and alive) with PDIL1 expression, progression-free survival (PFS) and overall survival (OS) were calculated using Kaplan-Meier analysis. Patients with lower levels of PDIL1 expression ( $< 6.0$ , the average score of all cases) had a significantly longer PFS compared with those with higher expression levels (Fig. 1B). Similarly, patients with lower expression had a longer survival (Fig. 1C). As shown in Table I, the parameters of age, risk stage, PDIL1 score, ratio of Ki-67 labeling and pathological subtypes also affected the OS as evidenced from the logistic regression analysis. The aforementioned data demonstrated that PDIL1 could be a prognostic indicator for patients with NSCLC.

*Combination treatment with Pem and <sup>125</sup>I inhibits cell viability and mobility.* Following the association of PDIL1 with NSCLC progression, the role of PDIL1 in tumor proliferation was subsequently explored. For this purpose, PDIL1 mRNA expression was investigated in H1299, H460 and A549 NSCLC cell lines and the PC6 SCLC cell line, using RT-qPCR to select the appropriate cell model for further experimentation. As presented in

Table I. Characteristics of patients with non-small cell lung cancer.

Clinicopathological factor	Number of patients (%)	OR
Sex		0.71
Male	50 (54.35)	
Female	42 (45.65)	
Age, years		1.39
<30	2 (2.17)	
30-60	51 (55.43)	
>60	39 (42.39)	
Prognosis		0.88
Alive	39 (42.39)	
Dead	53 (57.61)	
Risk stage		1.82
I	28 (30.43)	
II	49 (53.26)	
III	15 (16.31)	
PD-L1 IHC score		2.12
<6	33 (35.87)	
>6	59 (64.13)	
Ki-67, %		1.75
<10.0	28 (30.43)	
10.0-20.0	34 (36.96)	
>20.0	30 (32.61)	
Pathology		1.53
Squamous cell carcinoma	71 (77.17)	
Adenocarcinoma	16 (17.39)	
Large cell carcinoma	5 (5.43)	

OR, odds ratio.

Fig. 2A, among the four cell-lines, the relative mRNA expression of PD1L1 was significantly higher in H460 and A549 cells, but there was low expression in the H1299 cell line (~0.1-fold) and PC6 cell line (~0.22-fold), therefore the H460 and A549 cells would be utilized in the subsequent experiments. The expression of PD1L1 in fresh human NSCLC tissues was determined, and it was found to be significantly higher compared with that in normal tissue samples (Fig. 2B). To detect the anticancer effect of Pem and  $^{125}\text{I}$  on NSCLC cells, the MTT assay was performed using the aforementioned experimental groups, including the combination of Pem with  $^{125}\text{I}$ , Pem,  $^{125}\text{I}$  and DMSO as the control. As shown in Fig. 2C, the proliferation curves revealed that the combination of 2.0  $\mu\text{mol/l}$  Pem and radioactive  $^{125}\text{I}$  seeds significantly reduced H460 cells (left) and A549 (right) growth, compared with any of the single treatment groups. Although the inhibitory effects were observed in the Pem or  $^{125}\text{I}$  radiation single treatment groups, the suppression of proliferation was strongest in the combination treatment group, supporting the hypothesis that the combination of the two strategies could reduce tumor cell growth. To detect the effects of Pem+ $^{125}\text{I}$  on the migration ability of tumor cells, H460 and A549 cells were generated based on the above subgroups for 8 h and then the

concentrations of secreted MMP2 and MMP9 proteins were tested in the supernatant of NSCLC cell cultures by ELISA. As demonstrated in Fig. 2D and E, MMP2 secretion was suppressed more efficiently by Pem combined with  $^{125}\text{I}$  treatment group compared with that in the single treatment groups of Pem and  $^{125}\text{I}$ , and the control, for both cell lines. The secretion of MMP9 was also similarly inhibited by the combination treatment group compared with that in the single treatment groups in both cell lines (Fig. 2D and E). These data suggests that the combination of Pem and  $^{125}\text{I}$  played a critical role in repressing the tumor proliferation and aggressiveness.

*Combination treatment promotes cell apoptosis.* Apoptosis in H460 and A549 cells treated with the aforementioned reagents was determined using FCM analysis. As presented in Fig. 3A, the combination of Pem and  $^{125}\text{I}$  could induce tumor cell apoptosis up to ~65%, whereas the single Pem or  $^{125}\text{I}$  radiation treatment groups only induced apoptosis to <40%. According to cell proliferation mediated by the cell cycle, FCM was continuously performed to further detect the effect of the combination treatment on cell cycle by measuring the binding activity of PI. As shown in Fig. 3B, the combination treatment resulted in more H460 cells arrested in in S phase without ability to enter into the proliferation cycle and any of the single treatment analogously inhibited the blocking ability about 20%. Thus, combination with Pem and  $^{125}\text{I}$  showed the strong anti-tumor activity via suppressing the proliferation and mobility as well as promoting apoptosis.

*ADAM17 is downregulated by the combination treatment.* Following the observation that the combination of Pem and  $^{125}\text{I}$  was more effective in the NSCLC cell models compared with the single treatment groups, the underlying mechanisms involved in the anti-tumor effects were subsequently investigated. Based on the striking ADAM17 phenotype, the protein and mRNA expression levels of key proteins associated with apoptosis and proliferation, such as Bcl-2, Bax, p21 and p27 (20,21), in H460 cells treated with the aforementioned reagents were detected using western blot analysis and RT-qPCR. As presented in Fig. 4A, markedly decreased levels of Bcl-2 were observed in H460 cells following combination treatment compared with that in the single treatment groups. In addition, this combination also markedly upregulated Bax expression to induce the apoptosis in contrast with the single Pem or  $^{125}\text{I}$  treatment groups. Furthermore, the mRNA expression of p21 and p27 was determined using RT-qPCR, which are considered as regulators of the cell cycle (22,23). As shown in Fig. 4B, both p21 and p27 mRNA levels were significantly elevated in H460 cells (~40%) following the combination treatment, supporting the phenomenon that most of the tumor cells were arrested in S phase. Recently, ADAM17 was discovered as a crucial mediator of resistance to immunotherapy, therefore (24) the mRNA expression of ADAM17 was investigated. There was a significant reduction in ADAM17 levels in the combination treatment group compared with the control group (Fig. 4C), suggesting that the combination could modify the sensitivity of H460 cells to the targeted therapy and radiation. Therefore, these data demonstrate that the combination of Pem and  $^{125}\text{I}$  treatment suppressed NSCLC cell growth and induced the apoptosis through ADAM17 expression.

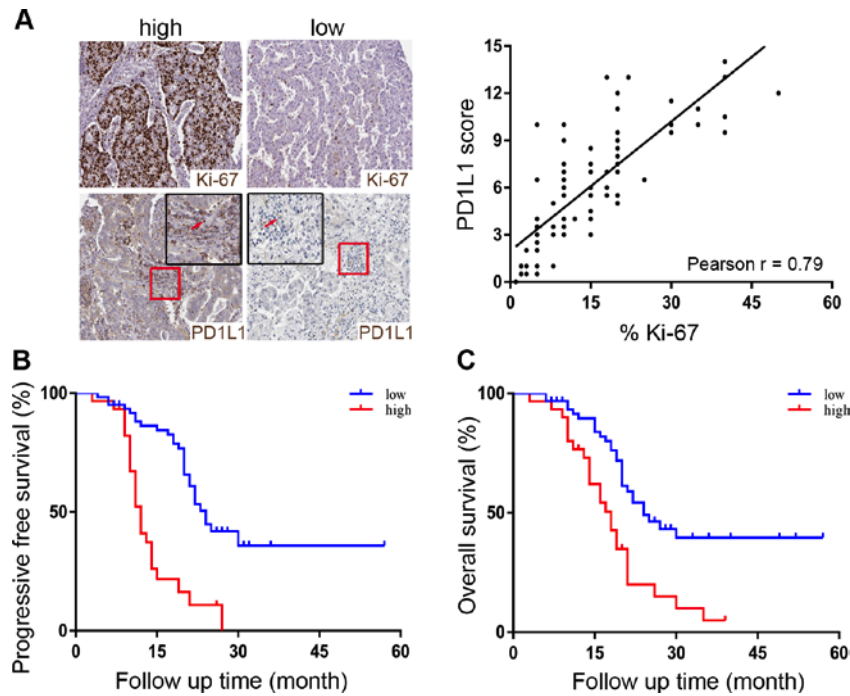


Figure 1. PDIL1 expression in NSCLC tissues and the association of PDIL1 with patient survival. (A) Representative IHC images of PDIL1 and Ki-67 expression in the high- and low-expressing groups (x100). The inset image shows the high-power field of PDIL1 expression (x400). The red arrows indicate PDIL1<sup>+</sup> cells. The positive correlation between PDIL1 score and Ki-67 index was analyzed using Pearson's correlation ( $P<0.0001$ ). The (B) progression-free survival and the (C) overall survival of patients with NSCLC divided into high- and low-expression groups, with respect to PDIL1 ( $P<0.0001$ ,  $P=0.0003$ ). PDIL1, programmed cell death 1 ligand 1; NSCLC, non-small cell lung cancer.

## Discussion

NSCLC is the leading cause of cancer-associated mortality globally (4). There are several types of NSCLC, including adenocarcinoma, squamous cell (epidermoid) carcinoma and large cell (undifferentiated) carcinoma. The prognosis and treatment options depend on the stage of the cancer, the subtype of lung cancer and the mutations of certain genes, such as the epidermal growth factor receptor (EGFR) gene or the anaplastic lymphoma kinase gene (25). The 5-year survival rate varies between 4 and 17%, relying on the cancer stage and geographical location (26). Neither items have been considered as the indicative biomarkers for diagnosis at early stage, nor have parameters been detected to be positively correlated with the clinicopathological features.

Different treatments are available for patients with NSCLC, including the standard therapy (operation combined with chemotherapy and radiotherapy). Immunotherapy exists as a strategy utilizing the host immune system to kill cancer cells, which is also called biotherapy. Immune checkpoint inhibitor therapy is now a popular choice for the treatment for numerous types of cancer, particularly NSCLC (27). PDIL1 is found to be upregulated in a wide array of malignancies, such as breast cancers and melanomas (28,29). Recent studies have discovered the medical roles of PDIL1/PD-1 protein in many malignancies, including lung cancer (30). Extending from the cancer cell surface, PDIL1 interplays with PD-1 on T cells. This coupling, known as an immune checkpoint, instructs the T cell to leave the tumor cell alone (31). Chemotherapy combined with atezolizumab (check point inhibitor) in the first-line treatment of extensive-stage SCLC led to significantly longer

overall survival and progression-free survival (32). Although immunotherapy, which targets PDIL1, is a common treatment option, the resistance to this strategy has gained more attention in recent years (31). Similar to the targeted therapy, resistance to the immunotherapeutic reagents can manifest through primary and existing therapies. A patient with primary resistance never responds to the immune therapy. With acquired resistance, a patient may initially respond, but this is often short-lived with eventual recurrence or metastases (33). In the present study the correlation between PDIL1 and clinicopathological characteristics and prognosis was firstly identified, and the combination therapeutic strategy, containing Pem and <sup>125</sup>I, was developed to subsequently investigate resistance of NSCLC cells to immunotherapy.

In the current study, PDIL1 was highly expressed in NSCLC compared with that in normal tissues. In addition, the NSCLC cases with high PDIL1 scores showed significant association to the proportion of Ki-67 index, indicating that PDIL1 contributed to the malignancy prediction. Moreover, dividing patients based on high or low expression revealed that patients with low expression levels were associated with poor prognosis of NSCLC, which supports that patients with high expression of PDIL1 relapse faster. Therefore, the expression of PDIL1 could be considered as a prognostic factor. Additionally, the *in vitro* studies with respect to the effects of the combination treatment of Pem and <sup>125</sup>I on the proliferation, invasion and apoptosis of NSCLC cells suggested that the combination strategy improved the resistance of tumor cells to the targeted PDIL1/PD-1 therapy via ADAM17 dysregulation. The combination of Pem with <sup>125</sup>I provides a novel approach to improve the resistance to immune checkpoint therapy

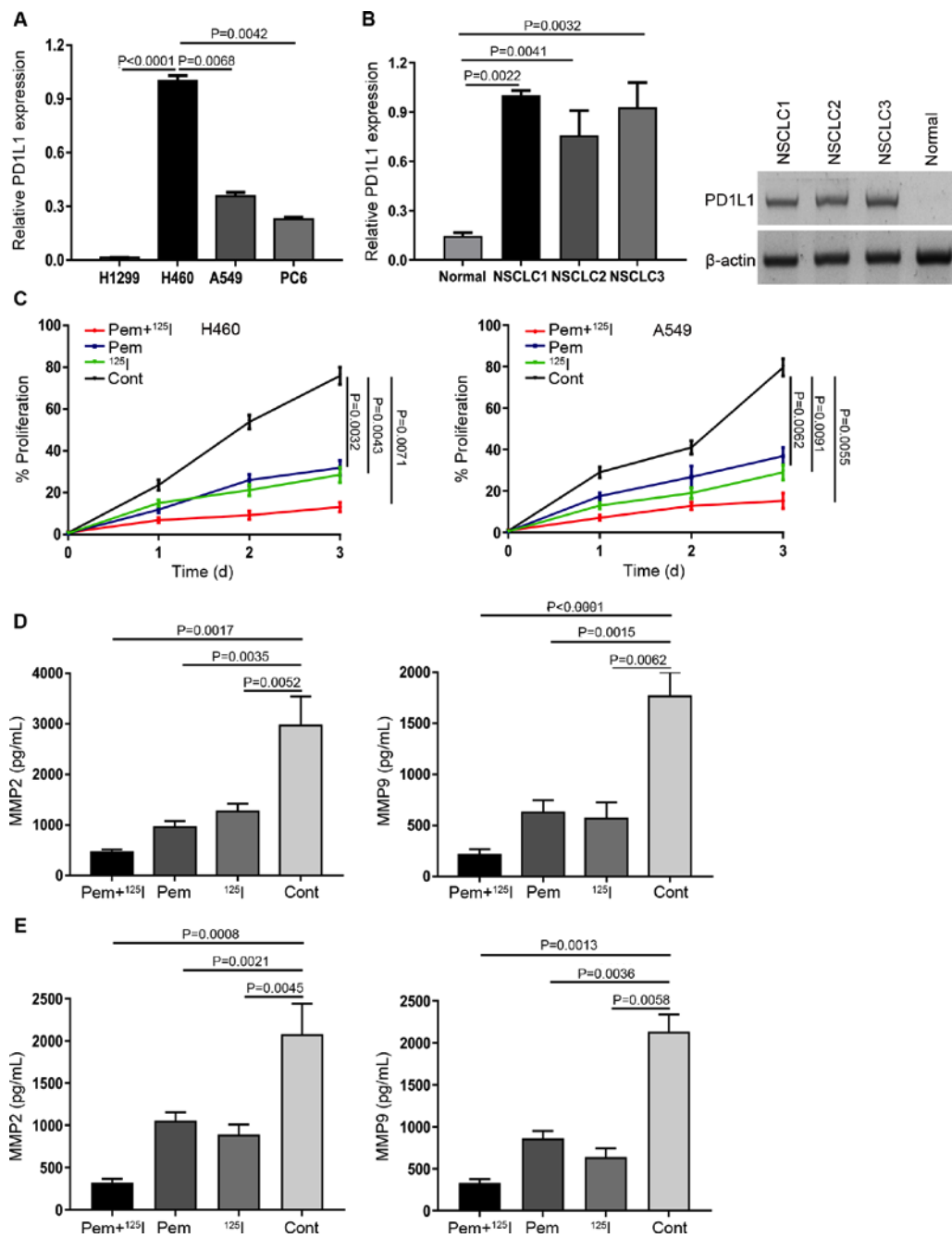


Figure 2. Effects of the combination of Pem and  $^{125}\text{I}$  on the proliferation and mobility in NSCLC cells. (A) The mRNA expression of PD1L1 in four cell lines examined using reverse transcription-quantitative PCR. (B) The PD1L1 mRNA and protein levels in fresh human NSCLC tissues. (C) H460 (left) and A549 (right) cells were treated with DMSO, and Pem and  $^{125}\text{I}$ , singularly or in combination for 24 h and the cell growth was measured using MTT assay. Amount of MMP2 (left) and MMP9 (right) released after (D) H460 and (E) A549 cells were incubated with DMSO, and Pem and  $^{125}\text{I}$ , singularly or in combination for 8 h was determined using ELISA. Pem, pembrolizumab; NSCLC, non-small cell lung cancer; PD1L1, programmed cell death 1 ligand 1; cont, control; MMP; matrix metalloproteinase; I, iodine.

among patients with NSCLC. Both Pem and  $^{125}\text{I}$  seed are widely used in clinical practice, which are safe and convenient for the patients. Additionally, the usage of internal radiation can successfully avoid excessive radiation exposure to the surrounding normal tissues. However, the combination with these two reagents inadvertently increases stress to the liver and affects renal function.

Upregulation of PD1L1 allows the cancer cells to avoid detection from the host immune system. The PD1L1/PD-1 complex in the tumor microenvironment plays a crucial role in tumor immune escape, which positively correlates with tumor

progression and development. Recent studies have revealed that the progression of cancer is partly attributed to the special tumor immune microenvironment (27). All cancer cells can avoid elimination by the host immune system via escaping immune surveillance and disrupting the immune checkpoint within ligand-receptor interaction (34). The cytotoxic T lymphocytes infiltrate the tumor microenvironment and specifically bind to tumor cells via ligand-receptor interaction, leading therefore to cancer cell death (31,35).

PD1L1/PD-1 signaling induces the evasion from immune surveillance using multiple specific mechanisms, as i) The

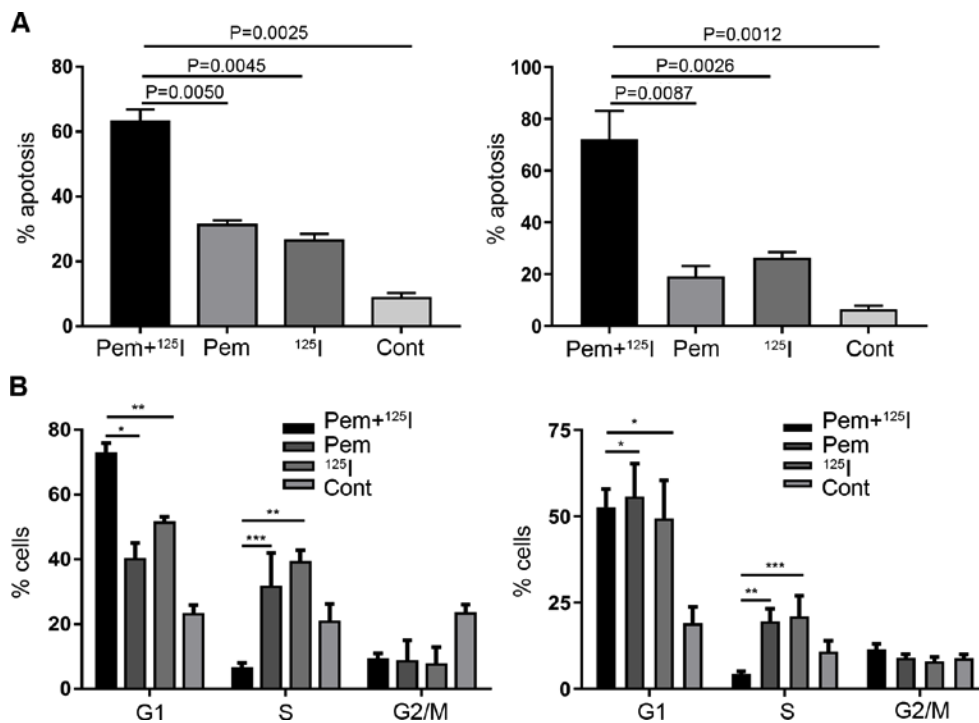


Figure 3. Effects of the combination of Pem and <sup>125</sup>I on apoptosis and cell cycle in non-small cell lung cancer cells. (A) Apoptosis and (B) cell cycle analysis using flow cytometry in H460 (left) and A549 (right) cells following treatment with control, and Pem and <sup>125</sup>I, singularly or in combination for 24 h. PD1L1, programmed cell death 1 ligand 1; Pem, pembrolumab; I, iodine; cont, control. \*P<0.05, \*\*P<0.01, \*\*\*P<0.001.

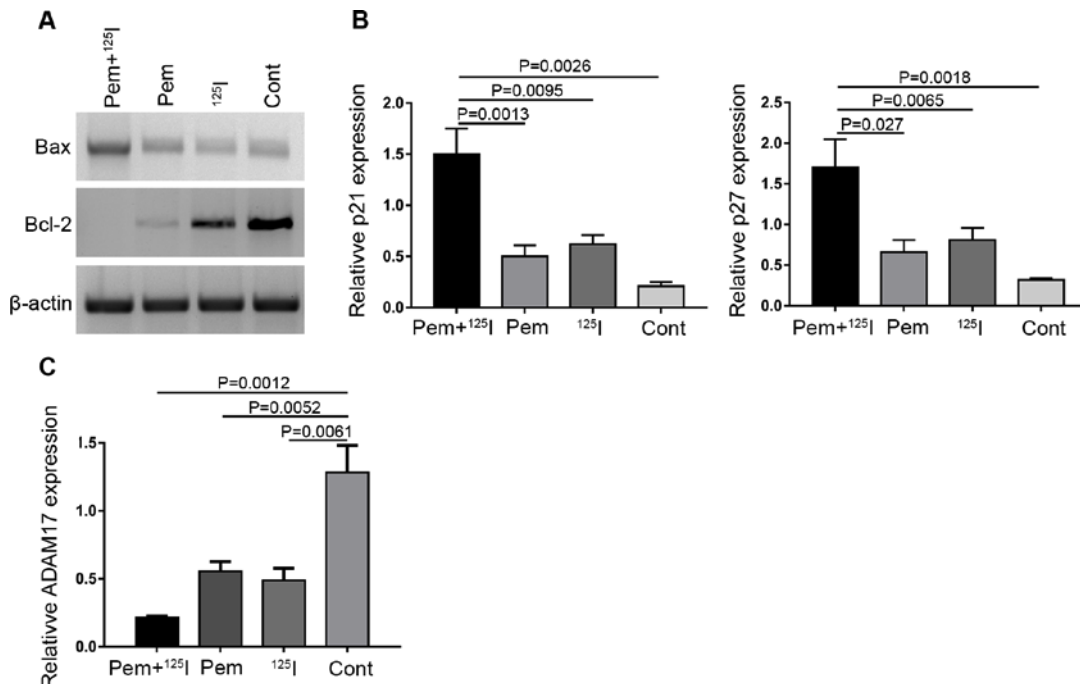


Figure 4. Protein and mRNA expression levels after Pem+<sup>125</sup>I functions. (A) Targeted effects of Pem+<sup>125</sup>I on the protein expression of Bcl-2 and Bax in H460 cells when incubated for 8 h, with DMSO, and Pem and <sup>125</sup>I, singularly or in combination, using western blot analysis. The β-actin protein was used as the internal control. The mRNA expression of (B) p21 (left) and p27 (right) and (C) ADAM17 in H460 cells using reverse transcription-quantitative PCR following the treatment with Pem+<sup>125</sup>I, Pem, <sup>125</sup>I and control for 8 h. (C) ADAM17, ADAM metalloproteinase domain 17; Pem, pembrolumab; I, iodine; cont, control.

exhaustion of tumor-infiltrating lymphocytes in tumor micro-environment is associated with PD1L1 expression of cancer cells (36); ii) PD-1 induces apoptosis of T cells by upregulating apoptotic genes, such as Bcl-2 and Bcl-xL (37); and iii) the down-regulation of mTOR, AKT, PTEN and ERK2 phosphorylation

by PD1L1/PD-1 signaling can induce regulatory T cells, thus suppressing the activity of effector T-cells (38).

A previous study has reported that higher PD1L1 expression was associated with more significant cancer aggressiveness based on the analysis of 196 cases with renal cell carcinoma (39),

consistent with the results from the present study. Over the last 4 years, a high number of PD1L1 small molecular inhibitors have been developed, which present promising results in clinical trials as immunotherapies (40-42). In general normal tissue, the immune response was restricted by the communications between transcription factors such as, paired box 8 and NF- $\kappa$ B with the goal of protecting normal tissue and limiting inflammation. However, among the cancers, PD1L1 expression can be induced by the loss of feedback restriction, which results in the ineffectiveness of systemic treatment when targeting PD1L1/PD-1 (43). Although PD1L1 targeted therapy has been reported to show effectiveness in targeting tumor cells, drug resistance is still a problem.

In the present study,  $^{125}\text{I}$  radiation was combined with Pem to reduce occurrence of drug resistance, which involved the downregulation of ADAM17. The ADAM family of proteins have been shown to promote invasion in different types of cancer, such as breast cancer, NSCLC and prostate cancer, which suggests that ADAM might be a promising therapeutic target (35). The major mechanism by which ADAM17 is hypothesized to promote these malignant properties involves activation of growth factors in the epidermal growth factor (EGF) family, such as pro-transforming growth factor- $\alpha$ , proheparin-binding EGF-like growth factor, amphiregulin or neuregulin (44). In particular, ADAM17 is a potential source of deregulation in the tumor microenvironment and adds an additional level of complexity to the manipulation of these natural systems, which also results in the resistance to chemo-/radiotherapy via the targeted signaling activation (45,46). ADAM17 can be considered as the therapeutic targeting when over activated in the tumor cells either alone or in combination with other treatment, including chemotherapy and radiotherapy (47,48). On the other hand, ADAM17 was discovered as a crucial mediator of resistance to radiotherapy, which can be considered as a therapeutic target when it overexpresses in tumor cells either alone or in combination with other immune modulating treatment. Upregulation of ADAM17 expression significantly contributes to pathogenesis of human cancers, such as the glioma and prostate cancer. ADAM17 has been known to induce activation of the EGFR/PI3K/Akt signaling, which plays a critical role in chemo-/radiotherapy resistance (49).

In conclusion, the current study discovered the crucial role of PD1L1 in NSCLC and reveals the relationship between clinicopathological characteristics and chemotherapeutic resistance. This data can be considered as the valuable diagnostic reference, which includes the expression of PD1L1 in NSCLC as a biomarker to predict the prognosis. A novel strategy regarding combination therapy in patients with NSCLC to solve the resistant problem and even expand this application to other malignancies with high levels of PD1L1.

## Acknowledgements

Not applicable.

## Funding

This study was supported by the Youth fund of the Second Hospital of Tianjin Medical University (grant no. 2017ydey09) and Opening grant in State Key laboratory of Molecular Vaccinology and Molecular diagnosis (grant no. 2017KF03)

## Availability of data and materials

The datasets used and/or analyzed during the current study are available from the corresponding author on reasonable request.

## Authors' contributions

SW and ZYG conceived and designed the experiments. SW, JZ and FJM performed the experiments. B.W. and YJY performed the pathological analysis of tissues. SW, ZYG and JZ contributed to the analysis and interpretation of data. FJM and SW wrote the manuscript. ZYG and JZ revised the manuscript for intellectual content.

## Ethics Approval and consent to participate

This study was approved by the Research Ethics Committee of Tianjin Medical University (Tianjin, China). All patients provided written informed consent in accordance with the Declaration of Helsinki.

## Patient consent for publication

Not applicable.

## Competing interests

The authors declare that they have no competing interests.

## References

1. Ferlay J, Soerjomataram I, Dikshit R, Eser S, Mathers C, Rebelo M, Parkin DM, Forman D and Bray F: Cancer incidence and mortality worldwide: Sources, methods and major patterns in GLOBOCAN 2012. *Int J Cancer* 136: E359-E386, 2015.
2. Horeweg N, van Rosmalen J, Heuvelmans MA, van der Aalst CM, Vliegthart R, Scholten ET, ten Haaf K, Nackaerts K, Lammers JW, Weenink C, *et al*: Lung cancer probability in patients with CT-detected pulmonary nodules: A prespecified analysis of data from the NELSON trial of low-dose CT screening. *Lancet Oncol* 15: 1332-1341, 2014.
3. Cedolini C, Bertozzi S, Londero AP, Bernardi S, Seriau L, Concina S, Cattin F and Risaliti A: Type of breast cancer diagnosis, screening, and survival. *Clin Breast Cancer* 14: 235-240, 2014.
4. Hirsch FR, Scagliotti GV, Mulshine JL, Kwon R, Curran WJ Jr, Wu YL and Paz-Ares L: Lung cancer: Current therapies and new targeted treatments. *Lancet* 389: 299-311, 2017.
5. Board PDQATE. Non-small cell lung cancer treatment (PDQ(R)): Health professional version. PDQ cancer information summaries. Bethesda (MD), National Cancer Institute (US), 2002.
6. Yatabe Y, Dacic S, Borczuk AC, Warth A, Russell PA, Lantuejoul S, Beasley MB, Thunnissen E, Pelosi G, Rekhtman N, *et al*: Best practices recommendations for diagnostic immunohistochemistry in lung cancer. *J Thorac Oncol* 14: 377-407, 2019.
7. Lin CK, Hsu YT, Christiani DC, Hung HY and Lin RT: Risks and burden of lung cancer incidence for residential petrochemical industrial complexes: A meta-analysis and application. *Environ Int* 121: 404-414, 2018.
8. Shukuya T and Carbone DP: Predictive markers for the efficacy of Anti-PD-1/PD-L1 antibodies in lung cancer. *J Thorac Oncol* 11: 976-988, 2016.
9. Garon EB, Rizvi NA, Hui R, Leighl N, Balmanoukian AS, Eder JP, Patnaik A, Aggarwal C, Gubens M, Horn L, *et al*: Pembrolizumab for the treatment of non-small-cell lung cancer. *N Engl J Med* 372: 2018-2028, 2015.
10. Gettinger S, Rizvi NA, Chow LQ, Borghaei H, Brahmer J, Ready N, Gerber DE, Shepherd FA, Antonia S, Goldman JW, *et al*: Nivolumab monotherapy for First-line treatment of advanced non-small-cell lung cancer. *J Clin Oncol* 34: 2980-2987, 2016.

11. Xia L, Liu Y and Wang Y: PD-1/PD-L1 blockade therapy in advanced non-small-cell lung cancer: Current status and future directions. *Oncologist* 24 (Suppl 1): S31-S41, 2019.
12. Reveiz L, Rueda JR and Cardona AF: Palliative endobronchial brachytherapy for non-small cell lung cancer. *Cochrane Database Syst Rev* 12: CD004284, 2012.
13. Li W, Dan G, Jiang J, Zheng Y, Zheng X and Deng D: Repeated iodine-125 seed implantations combined with external beam radiotherapy for the treatment of locally recurrent or metastatic stage III/IV non-small cell lung cancer: A retrospective study. *Radiat Oncol* 11: 119, 2016.
14. Woodard GA, Jones KD and Jablons DM: Lung cancer staging and prognosis. *Cancer Treat Res* 170: 47-75, 2016.
15. Chen BJ, Chapuy B, Ouyang J, Sun HH, Roemer MG, Xu ML, Yu H, Fletcher CD, Freeman GJ, Shipp MA and Rodig SJ: PD-L1 expression is characteristic of a subset of aggressive B-cell lymphomas and virus-associated malignancies. *Clin Cancer Res* 19: 3462-3473, 2013.
16. Nkomozepe P, Mazengenya P and Ihunwo AO: Age-related changes in Ki-67 and DCX expression in the BALB/c mouse (*Mus Musculus*) brain. *Int J Dev Neurosci* 72: 36-47, 2019.
17. Travis WD, Brambilla E, Nicholson AG, Yatabe Y, Austin JHM, Beasley MB, Chirieac LR, Dacic S, Duhig E, Flieder DB, *et al*: The 2015 World health organization classification of lung tumors: Impact of genetic, clinical and radiologic advances since the 2004 classification. *J Thorac Oncol* 10: 1243-1260, 2015.
18. Meng FJ, Wang S, Zhang J, Yan YJ, Wang CY, Yang CR, Guan ZY and Wang CL: Alteration in gene expression profiles of thymoma: Genetic differences and potential novel targets. *Thorac Cancer* 10: 1129-1135, 2019.
19. Livak KJ and Schmittgen TD: Analysis of relative gene expression data using real-time quantitative PCR and the 2(-Delta Delta C(T)) method. *Methods* 25: 402-408, 2001.
20. Zhu W, Li Z, Xiong L, Yu X, Chen X and Lin Q: FKBP3 promotes proliferation of non-small cell lung cancer cells through regulating Spl/HDAC2/p27. *Theranostics* 7: 3078-3089, 2017.
21. Liu G, Liu Z, Yan Y and Wang H: Effect of fraxetin on proliferation and apoptosis in breast cancer cells. *Oncol Lett* 14: 7374-738, 2017.
22. Abbastabar M, Kheyrollah M, Azizian K, Bagherlou N, Tehrani SS, Maniati M and Karimian A: Multiple functions of p27 in cell cycle, apoptosis, epigenetic modification and transcriptional regulation for the control of cell growth: A double-edged sword protein. *DNA Repair (Amst)* 69: 63-72, 2018.
23. Schafer KA: The cell cycle: A review. *Vet Pathol* 35: 461-478, 1998.
24. Pham DH, Kim JS, Kim SK, Shin DJ, Uong NT, Hyun H, Yoon MS, Kang SJ, Ryu YJ, Cho J, *et al*: Effects of ADAM10 and ADAM17 inhibitors on natural killer cell expansion and antibody-dependent cellular cytotoxicity against breast cancer cells in vitro. *Anticancer Res* 37: 5507-5513, 2017.
25. Bradbury P, Sivajohanathan D, Chan A, Kulkarni S, Ung Y and Ellis PM: Postoperative adjuvant systemic therapy in completely resected non-small-cell lung cancer: A systematic review. *Clin Lung Cancer* 18: 259-273.e8, 2017.
26. National Lung Screening Trial Research Team; Aberle DR, Adams AM, Berg CD, Black WC, Clapp JD, Fagerstrom RM, Gareen IF, Gatsonis C, Marcus PM and Sicks JD: Reduced lung-cancer mortality with low-dose computed tomographic screening. *N Engl J Med* 365: 395-409, 2011.
27. Sgambato A, Casaluce F, Sacco PC, Palazzolo G, Maione P, Rossi A, Ciardiello F and Gridelli C: Anti PD-1 and PDL-1 Immunotherapy in the Treatment of Advanced Non-small cell lung cancer (NSCLC): A review on toxicity profile and its management. *Curr Drug Saf* 11: 62-68, 2016.
28. Hautmann AH, Hautmann MG, Kölbl O, Herr W and Fleck M: Tumor-induced osteomalacia: An up-to-date review. *Curr Rheumatol Rep* 17: 512, 2015.
29. Weber J: Immune checkpoint proteins: A new therapeutic paradigm for cancer-preclinical background: CTLA-4 and PD-1 blockade. *Semin Oncol* 37: 430-439, 2010.
30. Şahin S, Batur Ş, Aydın Ö, Öztürk T, Turna A and Öz B: Programmed death-ligand-1 expression in non small cell lung cancer and prognosis. *Balkan Med J* 36: 184-189, 2019.
31. Velcheti V, Schalper KA, Carvajal DE, Anagnostou VK, Syrigos KN, Sznol M, Herbst RS, Gettinger SN, Chen L and Rimm DL: Programmed death ligand-1 expression in non-small cell lung cancer. *Lab Invest* 94: 107-116, 2014.
32. Horn L, Mansfield AS, Szczesna A, Havel L, Krzakowski M, Hochmair MJ, Huemer F, Losonczy G, Johnson ML, Nishio M, *et al*: First-line atezolizumab plus chemotherapy in extensive-stage small-cell lung cancer. *N Engl J Med* 379: 2220-2229, 2018.
33. Wang Q and Wu X: Primary and acquired resistance to PD-1/PD-L1 blockade in cancer treatment. *Int Immunopharmacol* 46: 210-219, 2017.
34. Thompson ED, Taube JM, Asch-Kendrick RJ, Ogurtsova A, Xu H, Sharma R, Meeker A, Argani P, Emens LA, Cimino-Mathews A, *et al*: PD-L1 expression and the immune microenvironment in primary invasive lobular carcinomas of the breast. *Mod Pathol* 30: 1551-1560, 2017.
35. Mullooly M, McGowan PM, Crown J and Duffy MJ: The ADAMs family of proteases as targets for the treatment of cancer. *Cancer Biol Ther* 17: 870-880, 2016.
36. Dong H, Strome SE, Salomao DR, Tamura H, Hirano F, Flies DB, Roche PC, Lu J, Zhu G, Tamada K, *et al*: Tumor-associated B7-H1 promotes T-cell apoptosis: A potential mechanism of immune evasion. *Nat Med* 8: 793-800, 2002.
37. Curiel TJ, Wei S, Dong H, Alvarez X, Cheng P, Mottram P, Kuchysiek R, Knutson KL, Daniel B, Zimmermann MC, *et al*: Blockade of B7-H1 improves myeloid dendritic cell-mediated antitumor immunity. *Nat Med* 9: 562-567, 2003.
38. Francisco LM, Salinas VH, Brown KE, Vanguri VK, Freeman GJ, Kuchroo VK and Sharpe AH: PD-L1 regulates the development, maintenance, and function of induced regulatory T cells. *J Exp Med* 206: 3015-329, 2009.
39. Thompson RH, Gillett MD, Cheville JC, Lohse CM, Dong H, Webster WS, Krejci KG, Lobo JR, Sengupta S, Chen L, *et al*: Costimulatory B7-H1 in renal cell carcinoma patients: Indicator of tumor aggressiveness and potential therapeutic target. *Proc Natl Acad Sci USA* 101: 17174-1779, 2004.
40. Haanen JB and Robert C: Immune checkpoint inhibitors. *Prog Tumor Res* 42: 55-66, 2015.
41. Izzedine H, Mateus C, Boutros C, Robert C, Rouvier P, Amoura Z and Mathian A: Renal effects of immune checkpoint inhibitors. *Nephrol Dial Transplant* 32: 936-942, 2017.
42. Doroshow DB, Sanmamed MF, Hastings K, Politi K, Rimm DL, Chen L, Melero I, Schalper KA and Herbst RS: Immunotherapy in non-small cell lung cancer: Facts and hopes. *Clin Cancer Res* 25: 4592-4602, 2019.
43. Caccese M, Indraccolo S, Zagonel V and Lombardi G: PD-1/PD-L1 immune-checkpoint inhibitors in glioblastoma: A concise review. *Crit Rev Oncol Hematol* 135: 128-134, 2019.
44. Rossello A, Nuti E, Ferrini S and Fabbi M: Targeting ADAM17 sheddase activity in cancer. *Curr Drug Targets* 17: 1908-1927, 2016.
45. Moss ML and Minond D: Recent advances in ADAM17 research: A promising target for cancer and inflammation. *Mediators Inflamm* 2017: 9673537, 2017.
46. Buchanan PC, Boylan KLM, Walcheck B, Heinze R, Geller MA, Argenta PA and Skubitz APN: Ectodomain shedding of the cell adhesion molecule Nectin-4 in ovarian cancer is mediated by ADAM10 and ADAM17. *J Biol Chem* 292: 6339-6351, 2017.
47. Wu J, Mishra HK and Walcheck B: Role of ADAM17 as a regulatory checkpoint of CD16A in NK cells and as a potential target for cancer immunotherapy. *J Leukoc Biol* 105: 1297-1303, 2019.
48. Wang R, Li Y, Tsung A, Huang H, Du Q, Yang M, Deng M, Xiong S, Wang X, Zhang L, *et al*: iNOS promotes CD24<sup>+</sup>CD133<sup>+</sup> liver cancer stem cell phenotype through a TACE/ADAM17-dependent Notch signaling pathway. *Proc Natl Acad Sci USA* 115: E10127-E10136, 2018.
49. Lan T, Wang H, Zhang Z, Zhang M, Qu Y, Zhao Z, Fan X, Zhan Q, Song Y and Yu C: Downregulation of  $\beta$ -arrestin 1 suppresses glioblastoma cell malignant progression via inhibition of Src signaling. *Exp Cell Res* 357: 51-58, 2017.